

# Stringer Panel Model for Structural Concrete Design



by Johan Blaauwendraad and Pierre C. J. Hoogenboom

*A large number of concrete structures can be treated as two-dimensional plate problems. Both the load and the support reactions have lines of action that coincide with the plane of the structure. This is how beams, walls, dapped beams, corbels, etc., are analyzed.*

*In practical design, two prominent methods of analysis exist: the strut-and-tie method and the finite element method. First, we will briefly discuss the advantages and disadvantages of these two methods, and subsequently introduce a new method called the stringer panel model for the design of economic and rational reinforcement. This approach takes into account both equilibrium and compatibility and has the advantage of being highly design-oriented. An additional advantage of this method is that an estimation of the crack width in the serviceability limit state is part of the result.*

**Keywords:** crack width and spacing; deep beams; finite element method; plates (structural members); reinforced concrete; structural design.

## RESEARCH SIGNIFICANCE

In current design practice, reinforcement is based on stresses calculated with linear elastic models. In this way we do not use the possibility of stress redistribution in statically indeterminate structures. The amount of reinforcement can be reduced when nonlinearities are taken into account, but the nonlinear finite element method can only be used for checking a final design because it is time-consuming and requires specialists in computational mechanics.

This paper presents a design model for structural concrete plates loaded in plane. It can be used for quickly analyzing the global nonlinear behavior of structures like deep beams, box-girder bridges, and caisson foundations. The model is based on a design concept that integrates the knowledge and experience of the designer with the ease of computational methods.

## STRUT-AND-TIE METHOD

A widely used approach in designing and dimensioning concrete structures is the strut-and-tie method (STM), also known as "truss analogy." The strut-and-tie method has a big advantage. The designer has to carefully consider the forces in the structure and choose an equilibrium system in which the load "flows" to the supports in a recognizable way. In this way the designer is able to insure that the specifications of the design are correct.

In spite of this some questions remain. Originally, the strut-and-tie method was based on the theory of plasticity. This theory guarantees safety when the structure is in equilibrium at all points. But the required redistribution of stress must be able to occur unrestrictedly; consequently, the structure needs to have sufficient deformation capacity. Herein lies the doubt. Is the structure as ductile as it is supposed to be? And if more than one equilibrium system is possible, which one is the best? These doubts are the reason that experimental verification of this method still continues. A good remedy can be to introduce in the analysis additional stiffness considerations. Such research is in progress. Another often recurring objection is that the redistribution of stress is accompanied by cracking and that the extent of deformation in a plasticity design is indeterminate. Thus, crack width prediction is not possible. According to the codes, the strut-and-tie method can only be applied in practice for the ultimate limit state (ULS) and not for the serviceability limit state (SLS). And if you do want to use the strut-and-tie method in the serviceability limit state, you must insure that the extent of cracking remains under control. One way to do this is to determine the elastic stress distribution and subsequently link up to that as closely as possible with the position of the struts and ties.

## FINITE ELEMENT METHOD

Finite element analysis (FEA) is a competitor to the strut-and-tie method. For the FEA approach, which is developed for computers, a number of programs are available, some of which are user-friendly. Such programs generate their own element grid and provide agreeable graphical output, all at an acceptable speed. Since computation times are no longer excessive, the designer can use fine meshes that will show every local stress peak. Some programs also offer a post-process option to translate the computed stresses into rein-

ACI Structural Journal, V. 93, No. 3, May-June 1996.

Received Apr. 27, 1994, and reviewed under Institute publication policies. Copyright © 1996, American Concrete Institute. All rights reserved, including the making of copies unless permission is obtained from the copyright proprietors. Pertinent discussion will be published in the March-April 1997 ACI Structural Journal if received by Nov. 1, 1996.

**Johan Blaauwendraad** is a professor of civil engineering at the Delft University of Technology, Delft, the Netherlands. He is active in IABSE Working Commissions. His research interests include computational methods for structural concrete.

**Pierre C. J. Hoogenboom** is a doctoral student at the Delft University of Technology, where he earned his MSc degree. He is currently developing the stringer panel model in a doctoral thesis study.

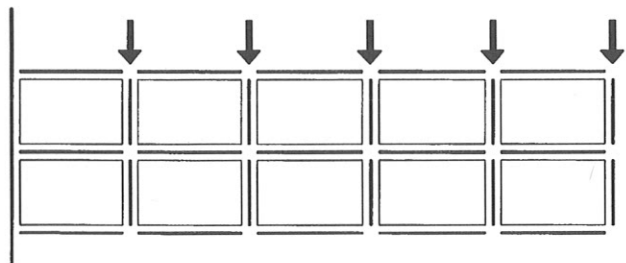


Fig. 1—Stylized model of airplane wing in old-time application of finite element method; stringers account for normal forces, rectangular panels transfer shear forces

forcement. Thus, a minimum effort provides the designer with a ready-to-use design. Little is left but to make the resulting reinforcement grid somewhat more practical.

Yet even with FEA some questions remain. The first concerns the ease offered by this method. The designer is hardly forced to think or develop a feel for the structural problem. This approach holds dangers of insufficiently considered and therefore dangerous details. The collapse of the Sleipner platform in 1991 clearly demonstrates this.<sup>1</sup> In this Norwegian offshore structure, failure is believed to have been caused by an uncritical choice of transverse shear reinforcement based on incorrect elastic stresses that resulted from a finite element analysis.

Another question concerns economy. Available postprocessors determine the reinforcement per element or per so-called integration point of an element from the stresses at that position. So the reinforcement follows the distribution of the elastic tensile stresses. This can lead to uneconomic reinforcement. For example, in the case of a slender beam loaded in bending, the elastic stress distribution is linear over the depth, and the lever arm between the resultant of the tensile stresses and the resultant of the compressive stresses is two-thirds of the height, or  $0.67 h$ . A standard postprocessor will base the reinforcement on this information. In reality, a designer will position all tensile reinforcement as far outward as possible, employing a bigger lever arm of about  $0.9 h$ . This results in a 25 percent reduction in reinforcement. From this point of view, postprocessors do not always give the best results. Control of crack width may be guaranteed, but there is a price to be paid.

### AN ALTERNATIVE: SPM

This article introduces an alternative that, in a way, combines the big advantage of the strut-and-tie method and the merits of the finite element method. As yet, this alternative has been developed for only orthogonal geometries where the edges of the considered structure are horizontal or vertical. An extension to random shapes is of later concern. Before going

into details, the three considerations that have lead to this alternative will be discussed.

### Distributed reinforcement

The first consideration is more the recognition of a fact. Although many plates are analyzed with struts and ties, the struts and ties are usually not recognizable as such in the resulting reinforcement. Generally, reinforcement consists of one or more concentrated tension bands situated near the edges, with intermediate reinforcement evenly distributed over the plate (or over large parts of it), often applied in two orthogonal directions.

### Behavior as shear panel

The second consideration is the results of tests carried out on uniformly reinforced panels. A lot of experimental research has been executed into the functioning of shear panels with distributed reinforcement either in one or both directions. Such panels appear to behave as a homogeneous continuum. A well-distributed pattern of cracks develops and the panels are still capable of transmitting shear stresses. The “modified compression field theory” and comparable other theories are available to determine the shear stiffness of the cracked reinforced panels loaded in shear.<sup>2</sup> So concrete plates with evenly distributed reinforcing could indeed be considered as shear panels.

### Remembering early times of FEM

The third consideration concerns developments of the finite element method in time. Presently, we are able to use the stiffness method for the analysis of very fine meshes. With the help of the computer thousands of equations can be solved quickly. But that was not always the case. During the end of the fifties and the beginning of the sixties, it was vital to work with as few unknowns as possible.

An effective means to limit the number of equations to be solved was the use of the force method. In this method, an equilibrium system was chosen along with a number of redundant stress parameters. Subsequently, the redundant stress parameters were calculated on the basis of deformation compatibility considerations. This force method has indeed been applied by, among others, aircraft companies to calculate airplane bodies and wings.<sup>3</sup> These airplane structures are “plate” structures consisting of regularly distributed stringers with thin skin plates (panels) attached in between. The essence of the early force method approach was to have the stringers transfer all normal forces and to assume that the panels could only transfer shear forces. Insofar as the panels also had stiffness against normal forces, this was (as a cooperative flange) attributed to the stringers. Fig. 1 shows a stylized example of such a wing.

The automatic choice of the correct redundant stress parameters appeared to be difficult and computation time-consuming, so the force method eventually had to give in to the stiffness method, which had been developed meanwhile, because the latter could far more easily be programmed into general purpose software.

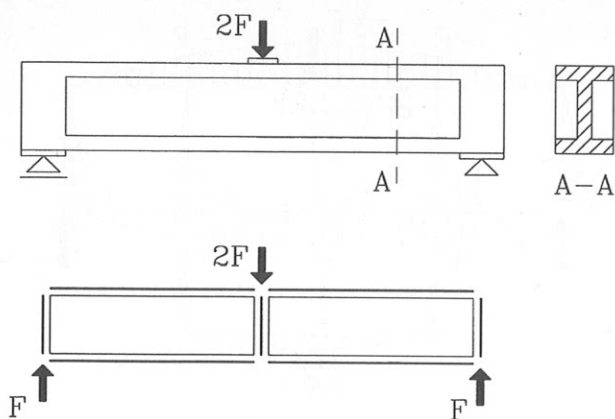


Fig. 2—Example of beam with I-shaped cross section modeled with stringers and panels; positions of stringers obvious

### Alternative

By now, the connection should be recognizable. Experimental research has established the shear capacity of reinforced concrete panels, and this shear panel concept fits well with the described force method approach for plates. Moreover, we know by now how to transform the force method into a stiffness method approach, as Blaauwendraad has shown.<sup>4</sup>

The proposed alternative is based on the idea that a structural concrete plate can be modeled into a system of linear horizontal and vertical stringers for the transfer of normal forces, whereas the rectangular fields in between can be filled with panels for the transfer of shear forces. The foregoing is called the stringer panel model (SPM).

Horizontal stringers can be easily indicated in beams with an upper and a lower flange (see Fig. 2). In these types of beams, vertical stringers always occur at the supports and where concentrated loads are applied.

When a structure has no flanges, the position of the stringers has to be judiciously estimated to take into consideration the center of the pressure zone and the place where the tensile reinforcement will be concentrated; Fig. 3 shows an example.

Quite another aspect is the width and the stiffness to be attributed to each of the stringers. Whether the structure still behaves elastically or has developed cracks determines which width should be assigned to each stringer. Axial stiffness for tensile members is derived from standard concrete mechanics knowledge. As for compression members, it is safe to assume relatively small widths, since the compression zone contracts heavily even in wall-type structures.

### EQUILIBRIUM SYSTEM OF SPM

Only a shear force occurs in the shear panel, and it has the same value  $v$  per unit length at all positions in the panel. This shear force  $v$  also works at the interface between the shear panel and the stringers bordering the panel. Then, according to equilibrium considerations, the normal force in a stringer increases or decreases linearly. Fig. 4 shows a drawing of this phenomenon for two horizontal stringers.

Two examples will now be discussed. The force distribution in the I-shaped beam in Fig. 2 is statically determinate,

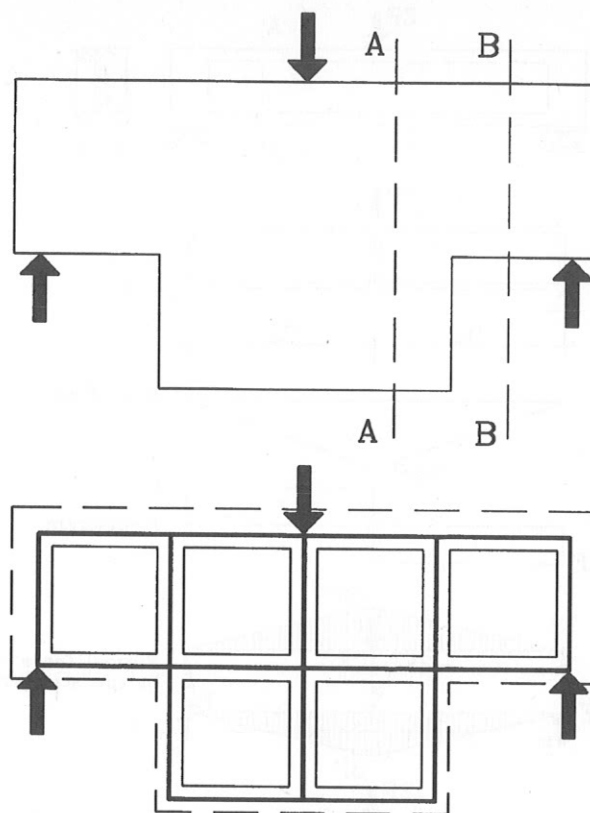


Fig. 3—Wall-type deep beam modeled with stringers and panels; position of stringers and panels must be judiciously determined

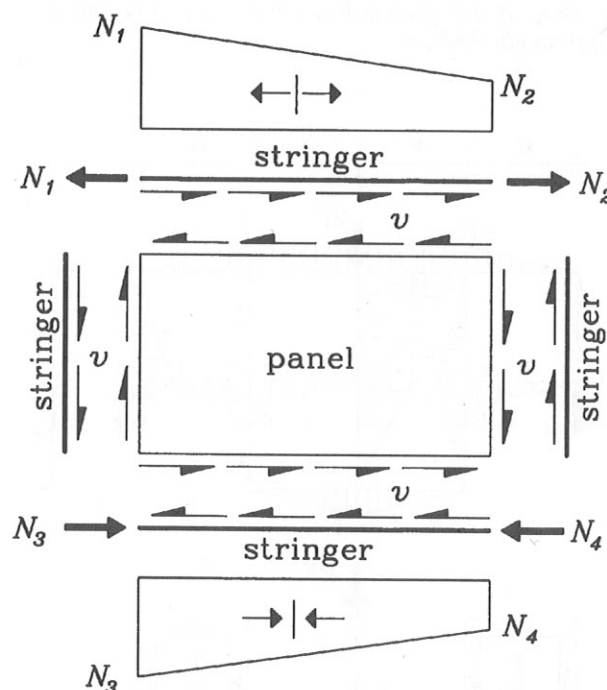


Fig. 4—On basis of equilibrium, normal force  $N$  in stringers develops linearly at constant shear force  $v$  per unit length at interface of panel and stringer

both externally and internally. In this case, the force distribution can be directly and uniquely derived from equilibrium. Fig. 5 shows the result. In all stringers, both horizontal and

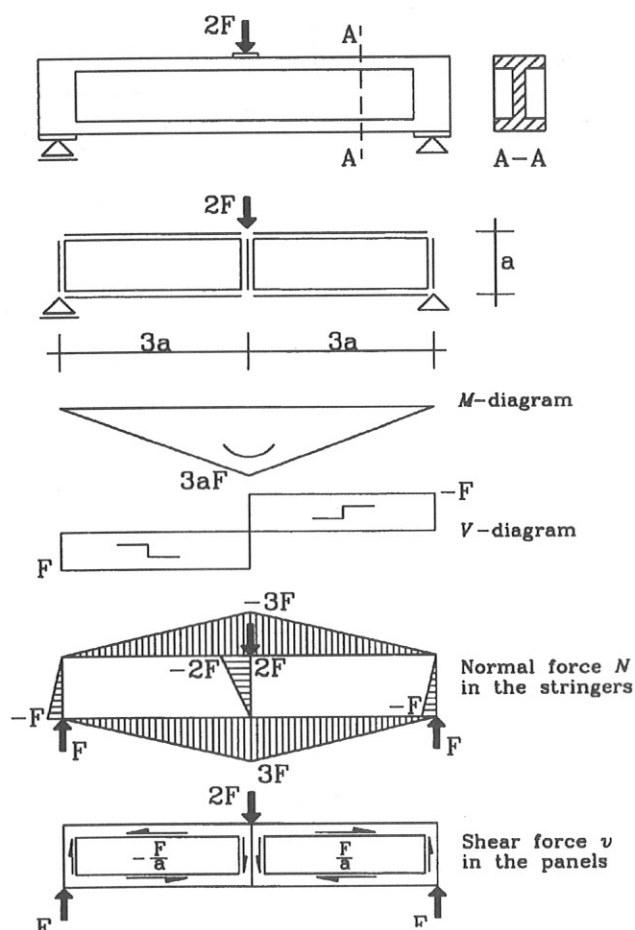


Fig. 5—Force distribution in beam of Fig. 2 can be uniquely derived from equilibrium

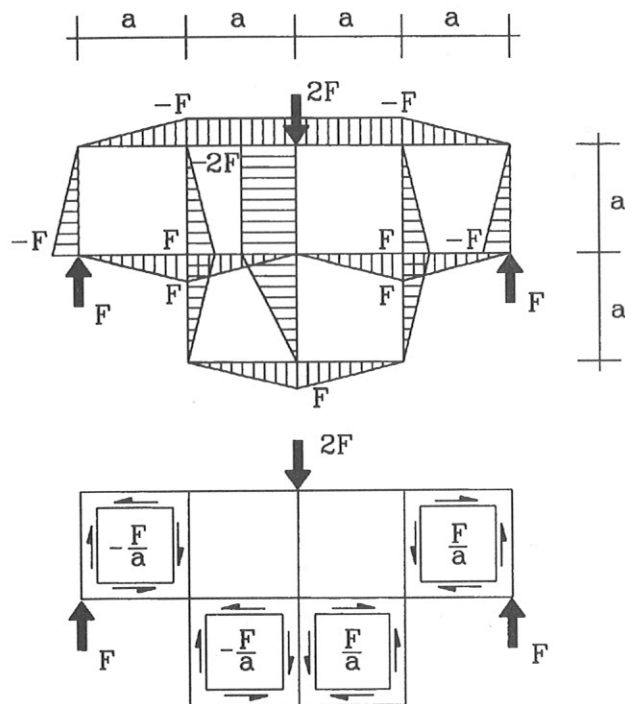


Fig. 6—Force distribution in deep beam of Fig. 3, supposing all shear force in middle part of deep beam carried by lower panels

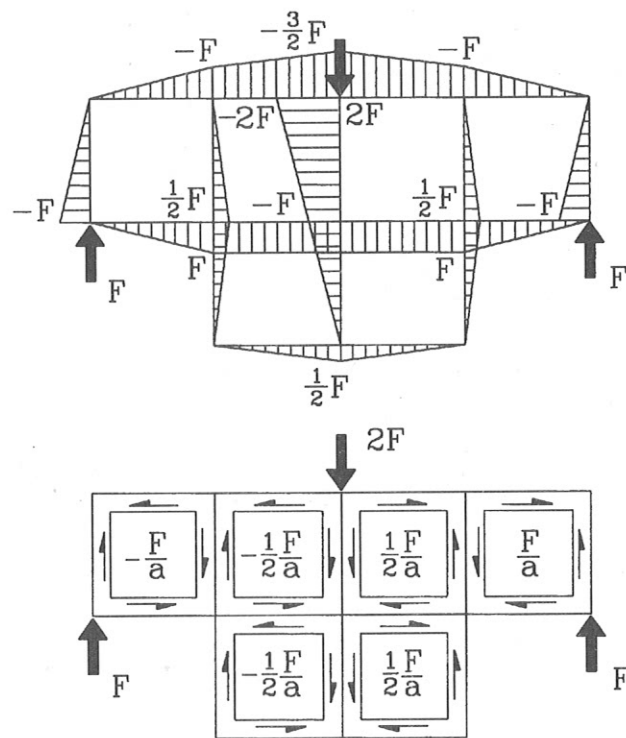


Fig. 7—Force distribution in deep beam of Fig. 3, supposing upper and lower panels contribute equally to transmission of shear force in middle part of beam

vertical, the normal force develops linearly from zero to a maximum value (either positive or negative). In this simple example, the normal force in horizontal stringers follows the development of the external bending moments. The normal forces in the vertical stringers appear as new aspects in relation to the classic beam theory. The constant shear force follows directly from the transverse shear force.

In the example of the wall in Fig. 3, the situation is less clear. Cross Section BB does not create any problems. The one panel in that cross section has to transmit all transverse shear force so that the shear force in the panel is fixed. But in Cross Section AA innumerable possibilities to spread the transverse shear force over the two panels in that cross section are available. An extreme supposition would be to assume that the lower panel does not carry anything. In that case, the problem can be compared to the problem in Fig. 2, and the stringers in the lower one-half of the wall will all remain without stress.

Another extreme supposition is that the lower panels carry all transverse shear force. This includes the stringer forces in Fig. 6. At midspan a maximum lever arm for the moment is present. Then the horizontal tensile force to be transmitted is  $F$ .

Fig. 7 shows the result of the intermediate situation when the transverse tensile force is uniformly distributed over the upper and lower panel. The sum of the horizontal tensile forces at midspan is now  $1.5 F$ . Fig. 8 shows the distribution of the horizontal stringer forces in the middle cross section.

On the basis of an equilibrium consideration alone, it is impossible to say which distribution is most probable. To be able to do that, the deformations also have to be taken into account.



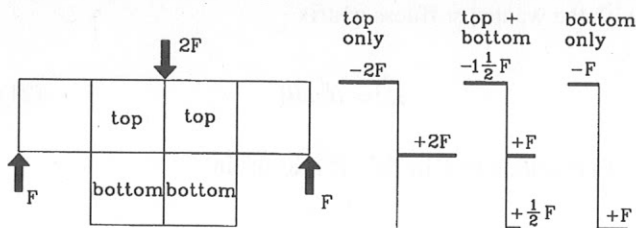


Fig. 8—At midspan, moment transmitted through normal forces in stringers; happens differently for various suppositions with regard to shear force

## ELASTIC STIFFNESS MATRIXES

This section has been included for the benefit of readers who are interested in the details of the finite element formulation of SPM. It can be passed over by readers who are just interested in the results of the new design method.

Elastic analysis can be done using a stiffness method approach,<sup>5</sup> although in reality an equilibrium stress state is used. The shear panel is given four degrees of freedom, as shown in Fig. 9. For a constant shear state, each edge will displace in its own direction and the displacement is the same for all positions on one edge. Four degrees of freedom are necessary, for the panel has three independent degrees for rigid body displacements. This results in one generalized deformation parameter that is related to the constant shear stress.

Three degrees of freedom are assigned to each stringer (see Fig. 9). These are the axial displacements at the two ends and an extra displacement in axial direction along the length of the stringer. This degree of freedom is associated with the interface force between the shear panel and the stringer. Formally speaking, this interface displacement is a Lagrange multiplier in the underlying variational principle. Three degrees of freedom are necessary to yield the desired linear distribution of the normal force, for the stringer has one rigid body displacement resulting in two generalized deformations that are associated with two parameters for the normal force.

### Panel

The shear panel has lengths  $a$  and  $b$  in the  $x$ - and  $y$ -directions, respectively. The thickness is  $t$  and the shear modulus  $G$ . Stiffness matrix  $K$  of the shear panel is derived from

$$K = B^T D B \quad (1)$$

Matrix  $B$  is the kinematic relation between generalized deformation  $e$  and displacement vector  $u$ , and  $D$  is the rigidity matrix connecting generalized deformation  $e$  and shear force  $v$  per unit length.

The one-half product of  $e$  and  $v$  is the total strain energy stored in the panel. From this we derive the relation between  $e$  and shear strain  $\gamma$

$$e = \gamma ab \quad (2)$$

Starting from the choice for vector  $u$

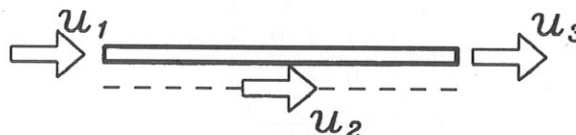
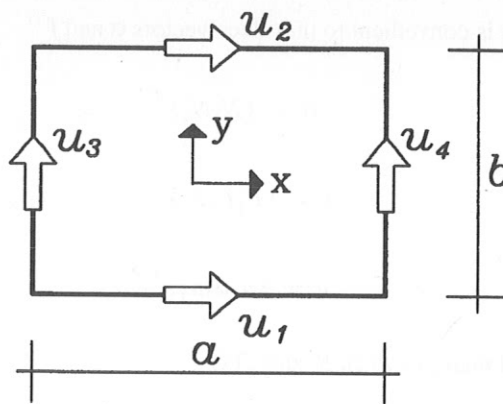


Fig. 9—Degrees of freedom in stringers and panels

$$u = \{u_1 u_2 u_3 u_4\}^T \quad (3)$$

we find

$$B = [-a \ a \ -b \ b] \quad (4)$$

$$D = \frac{Gt}{ab}$$

### Stringer

The stringer has length  $\ell$  and axial stiffness  $EA$ . This stiffness may vary along length  $\ell$ , so we write  $EA(x)$  in which the coordinate  $x$  origin is at the left end of the stringer. Again, the stiffness matrix will be derived in the form

$$K = B^T D B \quad (5)$$

Kinematic matrix  $B$  and rigidity matrix  $D$  are now derived applying the principle of minimum complementary energy

$$E_{compl} = \frac{1}{2} \int_0^\ell \frac{N^2(x)}{EA(x)} dx - F_1 u_1 - F_2 u_2 - F_3 u_3 \quad (6)$$

This energy expression will be minimized with respect to the two stress parameters  $N_1$  and  $N_2$ , which are the values of  $N(x)$  at both stringer ends. So we find the interpolation for  $N(x)$

$$N(x) = \left(1 - \frac{x}{\ell}\right) N_1 + \frac{x}{\ell} N_2 \quad (7)$$

and from equilibrium considerations we know

$$\begin{aligned} F_1 &= -N_1 \\ F_2 &= N_1 - N_2 \\ F_3 &= N_2 \end{aligned} \quad (8)$$

It is convenient to introduce vectors  $\sigma$  and  $f$

$$\sigma = \{N_1 N_2\}^T \quad (9)$$

$$f = \{F_1 F_2 F_3\}^T \quad (10)$$

$$u = \{u_1 u_2 u_3\}^T \quad (11)$$

and matrixes  $P(x)$ ,  $B$ , and  $C(x)$

$$P(x) = \begin{bmatrix} 1 - \frac{x}{\ell} & \frac{x}{\ell} \end{bmatrix} \quad (12)$$

$$B = \begin{bmatrix} -1 & 1 & 0 \\ 0 & -1 & 1 \end{bmatrix}$$

$$C(x) = \begin{bmatrix} 1 \\ EA(x) \end{bmatrix}$$

Using the contractions, we can write

$$N(x) = P(x) \sigma \quad (13)$$

$$f = B^T \sigma \quad (14)$$

Eq. (6) for  $E_{compl}$  can be written as

$$E_{compl} = \frac{1}{2} \sigma^T F \sigma - \sigma^T B u \quad (15)$$

in which flexibility matrix  $F$  is

$$F = \int_0^{\ell} P^T(x) C(x) P(x) dx \quad (16)$$

Minimizing  $E_{compl}$  with respect to  $\sigma$  yields

$$\frac{\partial E_{compl}}{\partial \sigma} = F \sigma - B u = 0 \quad (17)$$

In Eq. (17), both  $Bu$  and  $F\sigma$  can be interpreted as vector  $e$  of the generalized deformations

$$e = F \sigma \text{ and } e = B u \quad (18)$$

The condition of stationary complementary energy requires

$$\sigma = D B u \quad (19)$$

in which rigidity matrix  $D$  is equal to  $F^{-1}$ .

Substitution of Eq. (19) for  $\sigma$  in Eq. (14) between  $f$  and  $\sigma$  results in

$$f = K u \quad (20)$$

with the wanted stiffness matrix

$$K = B^T D B \quad (21)$$

Elaboration of  $F$  in Eq. (16) results in

$$F = \begin{bmatrix} \int_0^{\ell} \frac{\left(1 - \frac{x}{\ell}\right)^2}{EA(x)} dx & \int_0^{\ell} \frac{\left(1 - \frac{x}{\ell}\right) \frac{x}{\ell}}{EA(x)} dx \\ \int_0^{\ell} \frac{\left(1 - \frac{x}{\ell}\right) \frac{x}{\ell}}{EA(x)} dx & \int_0^{\ell} \frac{\left(\frac{x}{\ell}\right)^2}{EA(x)} dx \end{bmatrix} \quad (22)$$

In the case of constant axial stiffness  $EA$ , the flexibility and rigidity matrix become

$$F = \frac{\ell}{EA} \begin{bmatrix} \frac{1}{3} & \frac{1}{6} \\ \frac{1}{6} & \frac{1}{3} \end{bmatrix} \quad D = \frac{EA}{\ell} \begin{bmatrix} 4 & -2 \\ -2 & 4 \end{bmatrix} \quad (23)$$

In the case of a nonconstant  $EA(x)$ , the integrations have to be done numerically. The Simpson rule is chosen, which produces exact results in the limit case of constant stiffness.

## DESIGN OF REINFORCEMENT

In the horizontal and the vertical stringers, either compressive or tensile forces occur. Also, the transition from compression to tension may occur within a stringer. For compressive forces, compressive stress can be computed that will have to meet the requirements valid in the strut-and-tie method. The required reinforcement follows from the tensile forces. It will be concentrated in a narrow tension band.

The stress situation in the panels determines whether or not distributed structural wall reinforcement is required. This stress situation is established in the middle of the panel and the result is taken to be representative for the entire panel. What has to be determined is a membrane force  $n_{xx}$  in the horizontal direction, a membrane force  $n_{yy}$  in the vertical direction, and a shear force  $v_{xy}$ . The units for these three parameters are kN/m or kips/in. They can be derived by the modified compression field theory from strains  $\epsilon_{xx}$ ,  $\epsilon_{yy}$ , and  $\gamma_{xy}$  in the center of the panel.

With Mohr's stress circle, the main directions  $n_1$  and  $n_2$  of the membrane forces can be determined together with their direction. In case of tension, the cracking direction is also clearly perpendicular to the tensile stress.

A number of methods exist to design the distributed two-way net reinforcement from the panel forces  $n_{xx}$ ,  $n_{yy}$ , and  $v_{xy}$ . The question can be raised as to whether or not forces  $n_{xx}$  and  $n_{yy}$  have to be included in the consideration. In physical reality they are present, but in the analysis model they do not appear in the panel. This can be addressed in one of two ways. One way is to reinforce stringer elements for all normal forces  $N$  and panel elements just for shear forces  $v_{xy}$ . The normal force  $N$  in the stringer element results in concentrated

reinforcement and the shear force  $v_{xy}$  in the panel results in distributed reinforcement in two directions.

In the second way, we design the two-way panel reinforcement considering both shear force  $v_{xy}$  and normal forces  $n_{xx}$  and  $n_{yy}$ . In this case the concentrated reinforcement in the stringers can be reduced in proportion. Should the computation not lead to distributed reinforcement, often a minimum reinforcement, as indicated in the codes, will be applied.

## INFLUENCE OF CRACKING AND MODIFICATION OF REINFORCEMENT

The real axial stiffness of cracked reinforced tensile members will differ from the elastic stiffness. The same holds for the shear stiffness of the reinforced panels. Due to this, redistribution of stresses can take place in statically indeterminate structures after cracking. A computer program can take into account the change of stiffness by repeating the analyses with better approximations for the stiffnesses. A number of iteration steps may be needed per load level. When the load level is increased gradually, a complete load-displacement diagram can be computed for the structure and the failure load is determined. Either a compression stringer, a tension stringer, or a panel fails.

Cracked stringer stiffness can be determined by taking into account tension stiffening, as proposed in the Eurocode<sup>6</sup> (see Fig. 10). In the computer program, at the start of the analysis, the elastic  $EA$  is used. As a result, the linear distribution of  $N(x)$  along each stringer is found. At each cross section, the normal force  $N(x)$  determines the secant stiffness  $EA(x)$  that is a better approximation for the stiffness in the next iteration step. In the cracked state  $EA(x)$  will be a non-constant distribution, so the integrations in Eq. (22) must be done numerically. From this new flexibility matrix the stringer stiffness matrix in the cracked state is computed.

Shear stiffness is only computed in the center of the panel. At the end of each iteration step the strains  $\epsilon_{xx}$ ,  $\epsilon_{yy}$ , and  $\gamma_{xy}$  are known. The shear strain is an immediate result of the analysis and the normal strains are derived as the average of the adjacent stringers. Modified compression field theory tells us which forces  $n_{xx}$ ,  $n_{yy}$ , and  $v_{xy}$  are active in the panel at specified strains  $\epsilon_{xx}$ ,  $\epsilon_{yy}$ , and  $\gamma_{xy}$ . So the relation between  $n_{xy}$  and  $\gamma_{xy}$  is derived for given values of  $\epsilon_{xx}$  and  $\epsilon_{yy}$  (see Fig. 10). The ratio of  $v_{xy}$  and  $\gamma_{xy}$  is the new approximation for secant shear stiffness  $Gt$  in the next iteration step. From this shear stiffness the panel stiffness matrix in the cracked state is computed.

At the end of the analysis an ultimate load is found. If this load is sufficiently high, the design procedure is completed. Otherwise, we adapt the reinforcement adequately and restart the analysis. Experience indicates that the redistribution of stresses is small in wall-type structures, with the needed changes in reinforcement rather modest. Thus, the reinforcement that is based on the elastic stress distribution in the stringer panel model is a practical choice.

## CRACK WIDTH

Analysis produces average strains in stringers and panels, allowing determination of crack widths  $w$

$$w = ca\epsilon \quad (24)$$

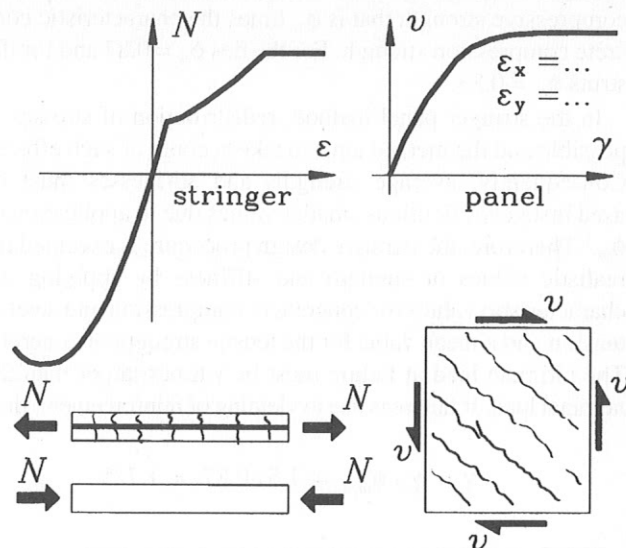


Fig. 10—After cracking, axial stiffness of stringers and shear stiffness of panels reduces

in which  $a$  is the crack spacing,  $\epsilon$  is the average strain, and  $c$  is a factor to account for the occurrence of small cracks beside the main crack (apply 0.74 for this factor). For average crack spacing, the Eurocode formula provides<sup>6</sup>

$$a = 50 + 0.25 \frac{d}{\rho} \quad (\text{mm}) \quad (25)$$

in which  $d$  is the average reinforcing bar diameter (mm) and  $\rho$  is the ratio of steel area and concrete area.

## VALIDATION OF MODEL

Results of the stringer panel model have been compared with test results for a series of slender beams in which bending is dominant, and a series of deep beams in which substantial shear deformation occurs.<sup>7</sup> The validation done so far shows that SPM predicts nonlinear load-displacement diagrams satisfactorily. Ultimate load, which is controlled by tension failure in the concentrated reinforcement due to yielding of steel, is also predicted accurately. It is not yet completely clear, however, if failure in the panel itself is adequately modeled. The authors will pay some more attention to this specific point.

Crack widths in the serviceability limit state are predicted well, provided that the structure has been properly reinforced; that is, with distributed reinforcement applied over the whole area of the wall or beam, accompanied by concentrated reinforcement as the main carrier of tensile forces.

## WHICH SAFETY CONCEPT?

Normal design practice for the strut-and-tie method is to apply a load factor  $\gamma_s$  to the nominal load and a partial safety factor  $\phi_m$  to the ultimate strength of the material. The nominal load is multiplied by  $\gamma_s$  and the strut-and-tie forces are determined on the basis of equilibrium for this ultimate load;  $\gamma_s = 1.5$  is adopted. The reinforcement area in the ties is computed from the tie forces found on the basis of a fictitious yield stress that is  $\phi_m$  times the characteristic yield

strength of steel. The struts are checked against a fictitious compressive strength that is  $\phi_m$  times the characteristic concrete compression strength. For the ties  $\phi_m = 0.87$  and for the struts  $\phi_m = 0.83$ .

In the stringer panel method, redistribution of stresses is possible and the method aims to take account of such effects. Consequently, average strengths and stiffnesses must be used instead of fictitious smaller values due to application of  $\phi_m$ .<sup>8</sup> Therefore, the iterative design procedure is executed for realistic values of strength and stiffness by applying the characteristic values for concrete in compression and steel in tension and a mean value for the tensile strength of concrete. The ultimate load at failure must be  $\gamma$  times larger than the nominal load. If failure is due to yielding of reinforcement, then

$$\gamma = \gamma_s / \phi_{m,s} = 1.5 / 0.87 = 1.725$$

If failure is due to compression in concrete, then

$$\gamma = \gamma_s / \phi_{m,c} = 1.5 / 0.83 = 1.8$$

If the reinforcement is chosen on the basis of the elastic stress distribution, no substantial redistribution is expected to occur. If the strength is reduced by  $\phi_m$ , then no large errors are made. In that case, the ultimate load has to be  $\gamma_s$  times the nominal load.

One may expect that the same amount of reinforcement will be found in both approaches. However, a substantial difference will occur in the computed crack widths. These will be smaller if realistic (higher) strengths and stiffnesses are used.

### APPLICATION

To demonstrate the potential of the stringer panel method, it is applied to a nontrivial structure. A wall with an opening is chosen that had been designed earlier with the strut-and-tie method and was published by J. Schlaich et al.<sup>9</sup> The structure, shown in the upper part of Fig. 11, is statically indeterminate. Schlaich et al. coped with this fact by considering two completely different truss models, assuming that each of them would carry one-half the load. They arrived at the reinforcement scheme shown in the lower part of Fig. 11.

The wall example of Fig. 3 bears parallels to this problem. The chosen stringer panel model is shown in Fig. 12. The panels have numbers 1 to 5. Nominal load  $F$  is 2000 kN (450 kips). At this load level  $\gamma_s = 1$ .

An elastic analysis in which the width of each stringer is calculated from each one-half-panel dimension adjacent to the stringer gives the elastic stress distribution shown in Fig. 13. Normal force diagrams are given for each stringer. The value of the panel shear forces are listed beside the figure (see Fig. 12 for panel numbers). These shear forces  $V$  are calculated as the product of  $v_{xy}$  in the panel and the height of the panel. Both stringer forces and panel forces are nondimensionalized by dividing them by  $\gamma_s F$ .

On the basis of these elastic stringer and panel forces the reinforcement has been chosen. The tensile stringer forces determine the concentrated reinforcement, and the shear forces form the basis of distributed two-way reinforcement.

The reinforcement areas are computed in the same way as STM. The nominal load is multiplied by  $\gamma_s = 1.5$  and the real yield stress is reduced by a factor  $\phi_m = 0.87$ . The reinforcement found in this way is shown in Fig. 14. Please note the strong reduction of the horizontal concentrated reinforcing bars from 7 to 3 in the center of the deep part of the wall.

Two nonlinear analyses are then carried out to compare against the elastic analysis and to determine crack widths. The first nonlinear analysis applies a reduced strength and stiffness that follows from the application of  $\phi_{m,s} = 0.87$ ,  $\phi_{m,c} = 0.83$  (compression), and  $\phi_{m,t} = 0.71$  (tension), although we think that this traditional approach is questionable. In this scenario, load factor  $\gamma_s$  must be increased to 1.5. As a consequence, the following data are used in this analysis:

#### Steel

$$f_{ys} = 434 \text{ MPa (62.9 ksi)}$$

$$E_s = 200,000 \text{ MPa (29,000 ksi)}$$

#### Concrete

$$f'_c = 17 \text{ MPa (2.47 ksi)}$$

$$f_{ct} = 2 \text{ MPa (0.29 ksi)}$$

$$E_c = 30,000 \text{ MPa (4350 ksi)}$$

The resulting stress distribution is presented in Fig. 15. The upper part of the figure shows the distribution at nominal load ( $\gamma_s = 1.0$ ) and the lower part shows the ultimate load ( $\gamma_s = 1.48$ ). Failure at  $\gamma_s = 1.48$  is due to yielding in the horizontal reinforcing bar bundle on top of the hole.

Redistribution due to cracking is very minimal. The force distributions at  $\gamma_s = 1.0$  and  $\gamma_s = 1.48$  do not differ noticeably from each other, nor from the elastic state. The reinforcement needs no further adaptation.

Maximum crack width at the wall center is 0.43 mm (0.017 in.) for the serviceability limit state and occurs at the horizontal bundle with three reinforcing bars.

The second nonlinear analysis repeats the process using the more realistic mean strength and stiffness:

#### Steel

$$f_{ys} = 500 \text{ MPa (72.5 ksi)}$$

$$E_s = 200,000 \text{ MPa (29,000 ksi)}$$

#### Concrete

$$f'_c = 20.4 \text{ MPa (2.96 ksi)}$$

$$f_{ct} = 4 \text{ MPa (0.58 ksi)}$$

$$E_c = 30,000 \text{ MPa (4350 ksi)}$$

Again, the reinforcement that follows from the elastic distribution of forces is applied. In this scenario the load factor  $\gamma_s$  must be incremented to 1.725 if failure is due to steel or to 1.8 if failure is due to concrete. The computed force distributions for  $\gamma_s = 1.0$  in the serviceability limit state and  $\gamma_s = 1.69$  in the ultimate limit state are shown in Fig. 16. Again, the differences with the elastic distribution are small. Factor 1.69 is surprisingly close to the quotient of the previously found  $\gamma_s = 1.48$  and  $\phi_{m,s} = 0.87$ .

Thus, for the example under consideration, the application of real strength and stiffness does not influence ultimate capacity. However, it does make a difference for the crack width. Now the maximum is 0.14 mm (0.006 in.), which is



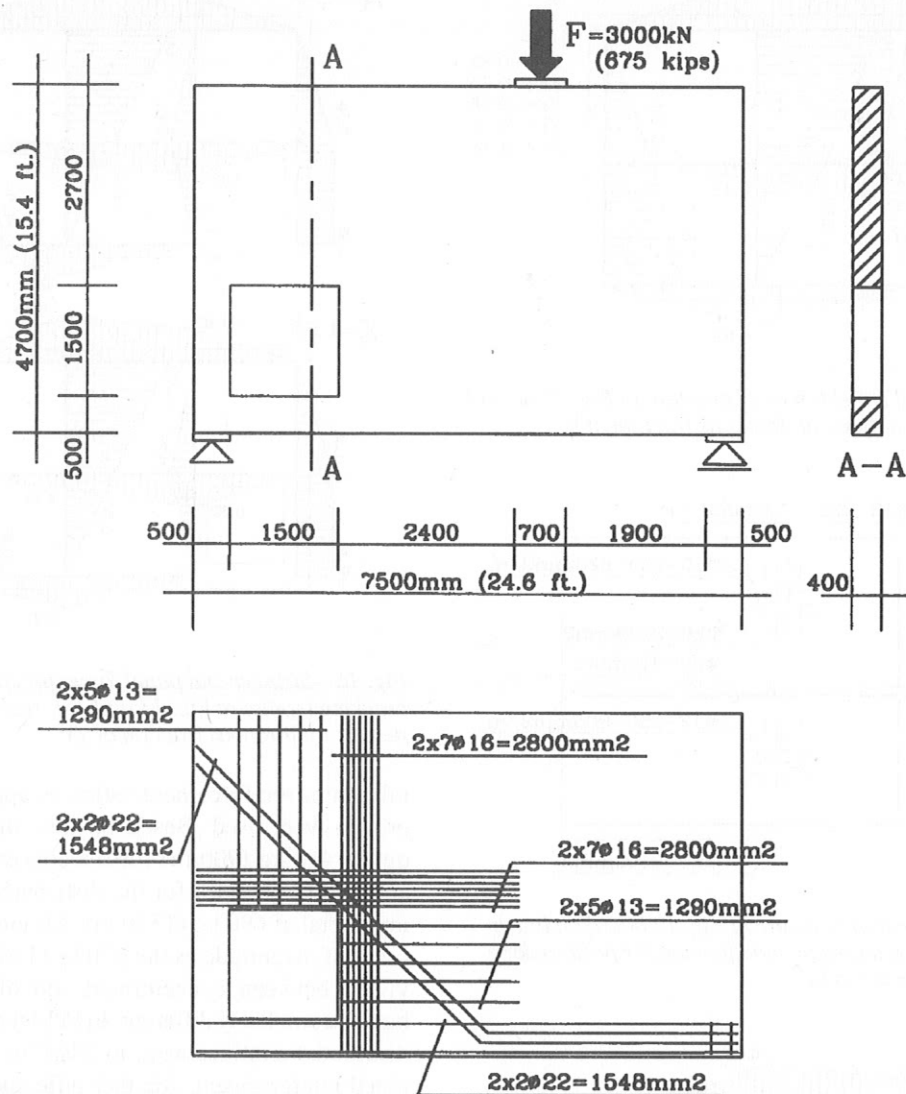


Fig. 11—Wall with opening and reinforcement as previously computed with STM by Schlaich et al. (100 mm = 3.94 in., 100 mm<sup>2</sup> = 0.155 in.<sup>2</sup>)

one-third of the previously found value of 0.43 mm (0.017 in.). This lower value is a far more realistic expectation for the crack width.

To better display this, Fig. 17 shows the  $N$ - $\epsilon$  diagram for a stringer that is loaded in tension for both realistic and reduced strengths and stiffnesses. Large differences in secant stiffness occur in the domain  $N > 300$  kN (67 kips).

For completeness, the load displacement diagrams for the structure are shown in Fig. 18. The choice of the more realistic average strength and stiffness yields a stiffer structure, which once more confirms the smaller crack widths.

Finally, the mass of reinforcement steel required by the scheme in Fig. 14 is 260 kg (580 lb) for the concentrated reinforcing bar and 410 kg (900 lb) for the distributed reinforcing bar, giving a total of 670 kg (1480 lb) for the SPM approach.

For comparison, the steel required by the STM approach was calculated based on the scheme shown in Fig. 11. For the distributed reinforcement, the same considerations for

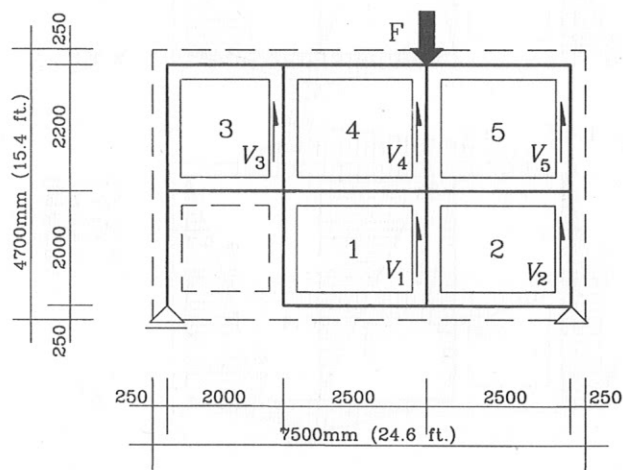


Fig. 12—Stringer panel model of structure in Fig. 11 (100 mm = 3.94 in.)

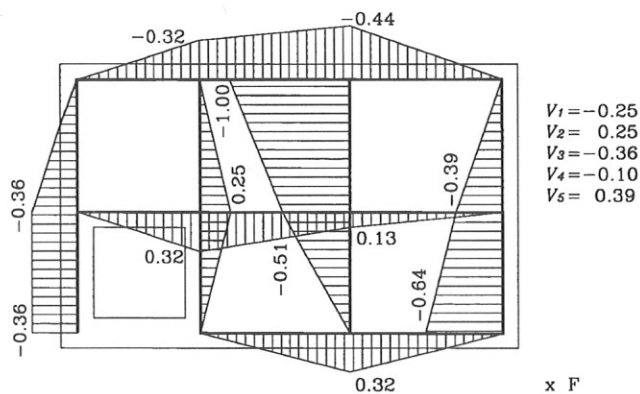


Fig. 13—Stringer and panel forces of structure in Fig. 12 according to linear-elastic analysis; all forces as fraction of  $F$

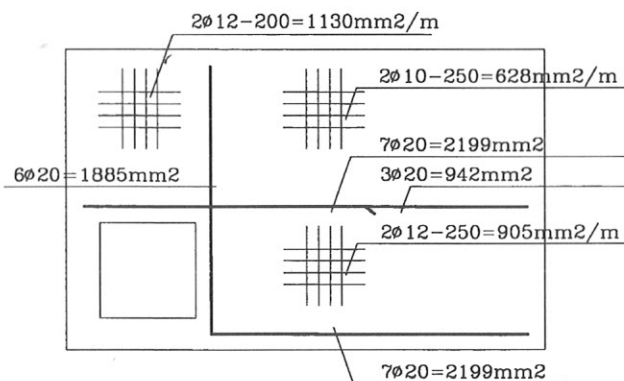


Fig. 14—Reinforcement in structure in Fig. 12 based on linear elastic SPM; scheme requires no modification for postcracking condition ( $100 \text{ mm}^2 = 0.155 \text{ in.}^2$ )

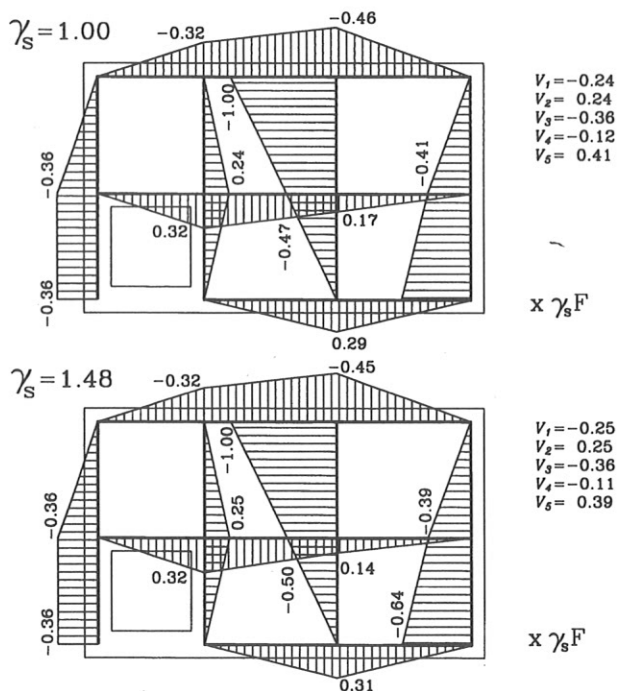


Fig. 15—Stringer and panel forces for structure in Fig. 12 after cracking (compare Fig. 13); reduced strengths and stiffnesses; all forces as fraction of  $\gamma_s F$

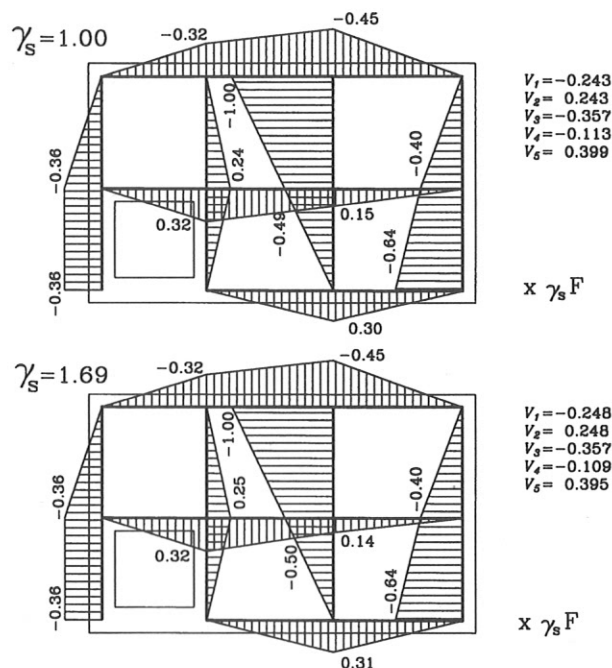


Fig. 16—Stringer and panel forces for structure in Fig. 12 after cracking (compare Fig. 13 and 15); realistic strengths and stiffnesses; all forces as fraction of  $\gamma_s F$

minimum reinforcement ratios as applied to the SPM approach were used. Based on this, the STM approach requires 410 kg (900 lb) for the concentrated reinforcement and 280 kg (620 lb) for the distributed reinforcement, giving a total of 690 kg (1520 lb). Although this is of the same order of magnitude as the 670 kg (1480 lb) for SPM, the division between concentrated and distributed reinforcing bars is completely different. In SPM the major part consists of distributed reinforcement. In STM the major part is concentrated reinforcement. Another difference is the length of the concentrated reinforcement at the top of the hole. The SPM approach recommends a much longer bundle than STM.

## CONCLUSION AND REFLECTION

The stringer panel model has potential to develop into a useful design tool for structural concrete. The method can be applied in parallel to the strut-and-tie method and to the design approach in which a postprocessor determines steel ratios based on a standard elastic fine mesh finite element analysis. It has special merits for nontrivial, statically indeterminate structures in which compatibility conditions are important. SPM takes an intermediate position between STM and FEA. The aim of SPM is a practical integration of structural design and computational modeling. As is the case with STM, the applicant of SPM has to behave as a designer. The designer makes decisions as to where to position the stringers and panels. The method can be made suitable for designing in a PC environment. The designer will no longer be troubled by the problem of which equilibrium system to choose (a difficulty encountered in applying STM to nontrivial structures), since an equilibrium system is found that meets the deformation constraints. Redistribution after cracking can occur, and the SPM model provides a useful in-

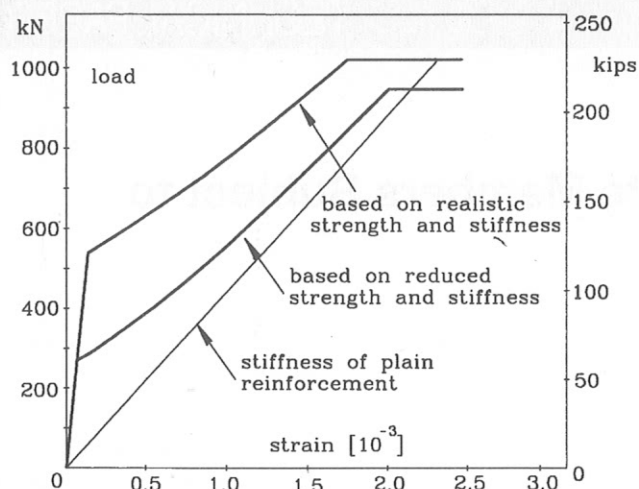


Fig. 17—N- $\epsilon$  diagram for concentrated reinforcement; secant axial stiffness depends strongly on choice for strengths and stiffnesses (realistic or reduced)

dication about the crack width in the serviceability limit state. The expectation for an elaboration of SPM is positive. The modeling of the behavior of stringers under tension and compression can be done quite well, with stiffness and ultimate capacity determined accurately. Similar progress for the shear panel is made. Nodes and compression stringers in SPM have to be inspected in a way that can be compared with STM.

The question of which category of reinforced concrete structures the proposed SPM is most suitable for is a valid one. It is best suited to wall-type structures. Also, spatial structures that are an assemblage of walls (such as caissons and box-shaped pier foundations) should lend themselves well to SPM analysis. Results so far show that SPM can also be used for beams and corbels, with and without flanges. It is felt that SPM will be an attractive method, next to STM and FEA, for a specific class of structural problems.

### FUTURE WORK

Further developments of the SPM concept are in progress. Two parallel tracks must be followed to improve the theory and to develop a design-oriented tool. The improvement of the theory means that gaps in knowledge must be filled in; among these is the prediction of failure in panels. To orient the method to structural designers, it must be offered to them as a design tool with a low level of complexity. Plans are to develop a computer-aided environment that facilitates

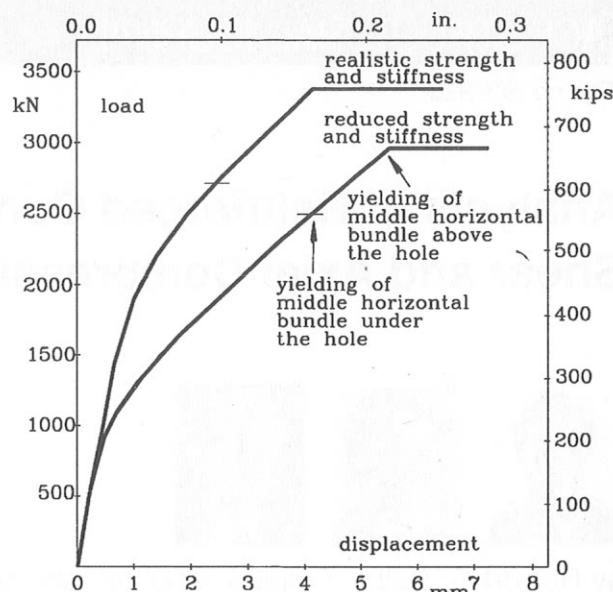


Fig. 18—Comparison of load displacement diagrams of structure for two different assumptions on strength and stiffness

design by drawing and analyzing in succession in an interactive way. The designer has the lead and makes decisions; the PC computes the consequences of these decisions and visualizes new results in a way familiar to the structural engineer.

### REFERENCES

1. Jakobsen, B., "Loss of the Sleipner A Platform," *Proceedings of the 2nd International Offshore and Polar Engineering Conference*, San Francisco, June 14-19, 1992, V. 1, pp. 1-8.
2. Vecchio, F. J., and Collins, M. P., "Modified Compression-Field Theory for Reinforced Concrete Elements Subjected to Shear," *ACI JOURNAL*, *Proceedings* V. 83, No. 2, 1986, pp. 219-231.
3. Argyris, J. H., "Energy Theorems and Structural Analysis," *Aircraft Engineering*, 1954 and 1955, reprinted by Butterworth's Scientific Publications, London, 1960.
4. Blaauwendraad, J., "Systematic Derivation of Continuous and Discrete Models in Structural Mechanics by Application of Direct Methods and Variational Principles," doctoral thesis, Delft University of Technology, 1973. (in Dutch)
5. Weaver, W., Jr., and Gere, J. M., *Matrix Analysis of Framed Structures*, Van Nostrand Reinhold, London, 1990.
6. "CEB-FIP Model Code 1990," *CEB Bulletin d'Information* No. 213/214, Lausanne, Switzerland, 1993.
7. Hoogenboom, P. C. J., "Stringer Panel Model," master's thesis, Delft University of Technology, 1993. (in Dutch)
8. Eibl, J., "Safety Considerations for Nonlinear Analysis," *Proceedings, IABSE Colloquium Structural Concrete*, Stuttgart, 1991.
9. Schlaich, J.; Schaefer, K.; and Jennewein, M., "Towards a Consistent Design of Structural Concrete," *PCI Journal*, V. 32, No. 3, 1987.